Title

Predicting fatal heat and humidity using the heat index model

Journal

Journal of Applied Physiology, 134(3)

ISSN

8750-7587

Authors

Lu, Yi-Chuan

Romps, David M

Publication Date

2023-03-01

DOI

10.1152/japplphysiol.00417.2022

Predicting fatal heat and humidity using the heat index model

Yi-Chuan Lu[12*] and David M. Romps[23]

[1]Department of Physics, University of California, Berkeley, USA
[2]Climate and Ecosystem Sciences Division, Lawrence Berkeley National Laboratory, Berkeley, USA
[3]Department of Earth and Planetary Science, University of California, Berkeley, USA
[*]Corresponding author. Email: yclu@berkeley.edu

Abstract

A unique wet-bulb temperature of 35°C is often used as the threshold for human survivability, but recent experiments have shown that a person's core temperature starts to rise at a wide range of critical wet-bulb temperatures. Here, it is shown that the model underlying the heat index correctly predicts those critical wet-bulb temperatures, explaining 95% of the variance in the values observed in laboratory heat-stress experiments. This is the first time the heat-index model has been validated against physiological data from laboratory experiments. For light and moderate exertion in an indoor setting, the heat index model predicts that the critical wet-bulb temperature ranges from 20 to 32°C, depending on the relative humidity, consistent with experimental results. For the same setting and exertion, the heat index model predicts fatal wet-bulb temperatures ranging from 24 to 37°C.

New & Noteworthy Recent experiments have identified the critical combinations of heat and humidity, in an indoor setting, above which an individual is unable to maintain a standard core temperature, indicating severe heat stress. It is shown here why this state of severe heat stress cannot be predicted using the wet-bulb temperature. Instead, it is shown that the recently extended heat index model can explain nearly all of the variance in the observed critical combinations of temperature and humidity, and can be used to calculate fatal combinations.

1 Introduction

It is been argued that humans cannot survive sustained exposure to a wet-bulb temperature T_w higher than a unique value of 35°C because such exposure would lead to a fatal core temperature (Sherwood and Huber, 2010). Subsequently, this T_w threshold has been used in many studies looking at survivability in global-warming scenarios (e.g., Pal and Eltahir, 2016; Schär, 2016; Im et al., 2017; Coffel et al., 2018; Im et al., 2018; Sherwood, 2018; Monteiro and Caballero, 2019; Raymond et al., 2020; Ramsay et al., 2021; Rogers et al., 2021; Saeed et al., 2021). On the other hand, Vecellio et al. (2022a) recently showed experimentally that the core temperature starts to rise (by accumulation of metabolic heat) not at a unique T_w but at a range spanning 26 to 30°C. Companion studies (Cottle et al., 2022; Wolf et al., 2022) found an even wider range of critical wet-bulb temperatures for subjects with different metabolic rates. These results motivate a search for more reliable predictors of heat stress and heat death.

Before building such predictors, it is important to distinguish between 1. the threshold for the core temperature to rise, as measured by Vecellio et al. (2022a), Cottle et al. (2022), and Wolf et al. (2022), and 2. the survivability threshold as defined by Sherwood and Huber (2010). The core temperature starts to rise when the accumulated metabolic heat brings the core temperature T_c above its healthy value of 37°C. An elevated core temperature is tolerable for fit and young adults as long as T_c remains at or below 38-39°C (Nybo and González-Alonso, 2015). On the other hand, a sustained core temperature of 41-42°C is a state of severe hyperthermia that is not generally survivable[1] (Bouchama and Knochel, 2002), and is therefore identified as the survivability threshold.

[1]Note that a heat-related fatality can occur for a variety of reasons. For example, the elevated skin blood flow that precedes

For obvious reasons, laboratory experiments do not intentionally induce core temperatures up to the threshold for survivability. Instead, human subjects are stressed only up to the point where their core temperature begins to rise above a standard temperature of 37°C (e.g., Vecellio et al., 2022a; Cottle et al., 2022; Wolf et al., 2022). To calculate what combinations of heat and humidity are fatal, we must extrapolate from the experimental data. Although Sherwood and Huber (2010) suggest that a core temperature of 41-42°C is induced at a wet-bulb temperature of 35°C, the fact that core temperatures begin to rise at a wide range of wet-bulb temperatures suggests that there is no unique fatal T_w.

In fact, we can understand from first principles why there is no unique T_w corresponding to heat stress or heat death. In a state of nakedness, profuse sweating, and a high rate of skin blood flow (pegging the skin temperature nearly equal to the core temperature T_c), the body has exhausted all of its thermoregulatory mechanisms. Ignoring respiratory ventilation for simplicity, a steady core temperature implies a balance between metabolism, radiation, and turbulent fluxes of sensible and latent heat,

$$Q - \sigma T_c^4 + \sigma T^4 - f(u)\left\{c_p(T_c - T_w) + L\left[q_v^*(T_c) - q_v^*(T_w)\right]\right\} = 0\,, \tag{1}$$

where Q is the metabolic heat generation per skin area, σ is the Stefan-Boltzmann constant, u is the wind speed and $f(u)$ is an effective mass flux of turbulent exchange between the skin and air, c_p is the heat capacity of air at constant pressure, L is water's specific latent heat of evaporation, $q_v^*(T)$ is the saturation mass fraction of water vapor, T is the temperature of the air and surroundings, and T_w is the wet-bulb temperature of the air. Consistent with the heat index model, which assumes a person is in the shade, there is no shortwave absorption here and the radiating surfaces are assumed to have the same temperature as the air. In equation (1), all the temperatures are understood to be the absolute temperatures, i.e., with units of kelvin.

We can now consider various limits for f. In a hypothetical scenario with no wind (i.e., not even natural convection, which is eliminated in zero gravity), f would be zero and the metabolic heat would need to be matched by net radiation. Therefore, in zero wind, there is a unique maximum temperature $T = (T_c^4 - Q/\sigma)^{1/4}$ that is compatible with a given steady-state core temperature T_c and metabolic rate Q. In the limit of infinite wind speed, f is infinite and there is a unique maximum wet-bulb temperature $T_w = T_c$ compatible with a given T_c. For a finite non-zero wind speed, there is no unique maximum T_w compatible with a given core temperature; instead, the maximum T_w is a function of Q and relative humidity (equivalently, a function of Q and T because the relative humidity can be calculated from T_w and T). These facts are illustrated in Figure 1, which plots the most thermally stressful combinations of T and T_w (for three different wind speeds u and two different metabolic rates Q) that are compatible with $T_c = 37°$ C. For $u = 0$ and a given Q, the solution to (1) is a locus of points at a single T. For $u = \infty$, the solution to (1) is a locus of points at a single T_w. For a given Q, it is only in the limit of infinite wind speed that there is a unique maximum T_w (equal to T_c) that is compatible with a core temperature of T_c, regardless of Q and relative humidity; for all finite wind speeds, the maximum T_w is a function of both Q and relative humidity. Therefore, there should be no single T_w that predicts when the core temperature will rise above a standard value of 37°C, and no single T_w that corresponds to fatal conditions of T_c = 41-42°C.

Indeed, as shown in the recent empirical studies, the wet-bulb temperature at which humans begin to have elevated core temperatures varies from person to person and with different levels of exertion. To capture this variability, we must use a model of a human's core temperature that incorporates the metabolic rate, ambient temperature and humidity, and the wind speed. For this purpose, we use the model of thermoregulation that underlies the heat index (Steadman, 1979; Lu and Romps, 2022). In the next section, we describe the how this thermoregulation model is built and illustrate how this model can be used to define an index for heat stress.

2 The heat index model

Humans use several behavioral and physiological strategies to maintain their core temperature T_c at or close to its standard value of 37°C. The model underlying the heat index makes the simplifying assumption that

an elevated core temperature stresses the cardiovascular system, and heart failure can occur in advance of the fatal core temperature (Gostimirovic et al., 2020). Therefore, a core temperature of 41-42°C is a conservative threshold for survivability, applicable to young, healthy adults.

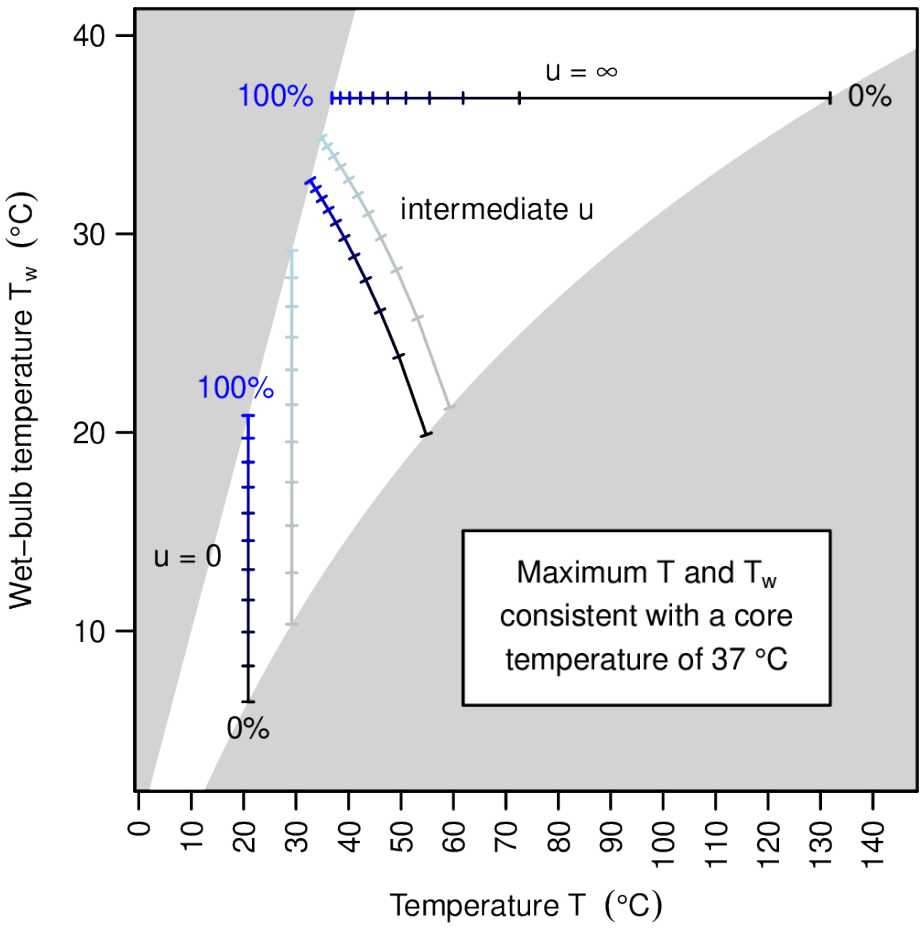

Figure 1: Maximum temperature T and wet-bulb temperature T_w that are compatible with a core temperature of $T_c = 37°\mathrm{C}$, plotted for three different wind speeds. For each locus of points, the tick marks indicate 10% increments of relative humidity, ranging from (black) 0% to (blue) 100%. The three black-and-blue curves show the loci of points for a metabolic heat production of $Q = 100$ W m^{-2}. The grey-and-light-blue curves show the same for $Q = 50$ W m^{-2}; the grey-and-light-blue $u = \infty$ curve is hidden underneath the black-and-blue $u = \infty$ curve, which is independent of Q. The two greyed-out regions denote pairs of T and T_w that are unphysical because they would imply a relative humidity greater than one or less than zero.

those strategies form a one-dimensional space (Steadman, 1979; Lu and Romps, 2022), i.e., that the different strategies are deployed one after another as opposed to in parallel. For example, in extremely cold conditions, the clothing is infinitely thick and the human chooses only what fraction of the skin to leave exposed. In cold and mild conditions, the area of exposed skin is held constant, but the thickness of clothing is varied. In hot conditions, the clothing thickness is set to zero, but the skin blood flow is modulated. In extremely hot conditions, the skin blood flow is infinite[2], so all thermoregulatory strategies have been exhausted, but the thermoregulatory state can be quantified by the temperature above 37°C at which the core equilibrates.

Because the various strategies are used sequentially, a single real number can be used to encode four pieces of information: the area of exposed skin (which varies only in what Lu and Romps, 2022, called region I), the clothing thickness (varies only in regions II and III), skin blood flow (varies only in regions IV and V), and the equilibrium core temperature (varies only in region VI). There are an infinite number of ways to map this set of strategies, or thermoregulatory states, to a real number. A particularly convenient choice is to map each state to the air temperature that, when combined with a set of commonly experienced reference values for vapor pressure, wind speed, and metabolic rate, would cause a human to adopt that state. This mapping is called the apparent temperature T_a and was defined by Steadman (1979) using a reference vapor pressure of $p_{v0} = 1.6$ kPa, a reference wind speed of $u_0 = 1.5$ m s^{-1}, and a reference metabolic rate of $Q_0 = 180$ W m^{-2}. Given this definition of apparent temperature, the thermoregulation model gives us the function $T_a\left(T, p_v, u, Q\right)$. Note that the apparent temperature satisfies the identity $T_a(T, p_{v0}, u_0, Q_0) = T$.

The heat index is a special case of the apparent temperature in which the arguments u and Q are replaced by their reference values of 1.5 m s^{-1} and 180 W m^{-2}, respectively. In other words, the heat index HI is defined as

$$\mathrm{HI}(T, p_v) = T_a\left(T, p_v, u_0, Q_0\right) . \tag{2}$$

Therefore, the heat index should be used with care as it is the apparent temperature for the observed temperature and vapor pressure, *but assuming the human has a metabolic rate of 180 W m^{-2} and is in a breeze of 1.5 m s^{-1}*. In this work, we will use the more general apparent temperature to explain the empirical data from Vecellio et al. (2022a), Cottle et al. (2022), and Wolf et al. (2022) because their experiments were conducted at various metabolic rates (all below 180 W m^{-2}) in a room with a wind speed much smaller than 1.5 m s^{-1}. Nevertheless, we will use the same model of thermoregulation that underlies the definition of the heat index.

By construction, the equilibrium core temperature is a function of apparent temperature T_a: for apparent temperatures below 71.5 °C, the equilibrium core temperature is 37 °C[3], but it rises monotonically with higher apparent temperatures, as shown in the top panel of Figure 2. At an apparent temperature of 93.3 °C, the core temperature equilibrates at 42 °C, which is considered a fatal value if sustained[4]. These two apparent temperature thresholds are labeled in Figure 2. This curve, mapping apparent temperature to equilibrium core temperature, is invariant with respect to the metabolic rate: all else equal, a higher metabolic rate will move a person to the right on this curve, but will not change the curve itself.

Since the human body has thermal inertia, a sudden exposure to an apparent temperature at or beyond 93.3 °C does not immediately bring the core to 42 °C. Instead, the time it takes the core to reach 42 °C depends mainly on the apparent temperature and wind speed. The bottom panel of Figure 2 plots this

[2]The model underlying the heat index is an idealization in several regards, including its assumption that humans can have an infinite skin blood flow. Lu and Romps (2022) showed that imposing a realistic upper bound for the skin blood flow introduces, at most, minor corrections to the heat index at the expense of introducing an additional parameter. For the experiments in Wolf et al. (2022) that will be discussed in this work, imposing a realistic upper bound would change the predicted equilibrium core temperature by less than 0.5°C.

[3]In the heat-index model, the core temperature stays constant until the body's metabolic heat becomes uncompensable at the apparent temperature of 71.5 °C. This differs from some other thermoregulation models (e.g., Stolwijk and Hardy, 1966) that have an "active" system in which the skin blood flow and sweating rate are sensitive functions of the core and/or skin temperatures. In those active models, the core temperature would rise slightly above 37 °C to trigger the necessary vasodilation and sweating even before the apparent temperature exceeds 71.5 °C. The heat-index model is built as a "passive" system, in which these sensitive relationships are approximated by diagnostic relationships, which set the skin blood flow and sweating rate at the values needed to keep the core temperature at 37 °C.

[4]Temperatures of 71.5 and 93.3 °C might sound absurdly high, but these are calculated using the original convention of Steadman (1979), who defined the heat index with respect to a reference water-vapor pressure of 1.6 kPa. At that water-vapor pressure, 71.5 °C has a relative humidity of 5% and a wet-bulb temperature of only 30.0 °C. Likewise, 93.3 °C has a relative humidity of 2% and a wet-bulb temperature of only 34.1 °C. With the reference wind speed of 1.5 m s^{-1}, the enormous latent heat of water vapor enables the temperature of a wetted surface, or a sweaty human, to be much lower than the dry-bulb temperature. See the Appendix for a related discussion of practical limits on the sweating rate.

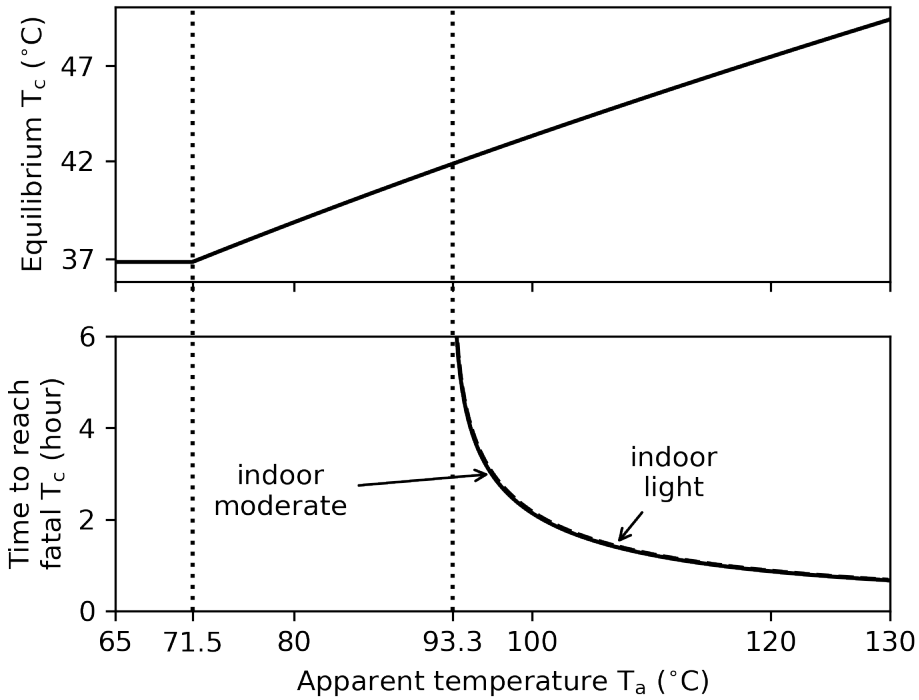

Figure 2: (top panel) The equilibrium core temperature as a function of the apparent temperature T_a. The dashed vertical lines mark the thresholds of 71.5 °C (core temperature begins to rises) and 93.3 °C (core temperature would equilibrate at 42 °C). (bottom panel) The time it takes the core to reach the fatal value of 42 °C for the wind speed of 0.2 m s^{-1}. These curves have a very weak, almost imperceptible, dependence on the metabolic rate: the dashed curve is for $Q = 82.9$ W m^{-2} (the mean value for the "light" exertion group defined in the next section) and the solid curve is for $Q = 133$ W m^{-2} (the mean value for the "moderate" exertion group).

"time to death" as a function of apparent temperature for two different cases considered in the next section: "light" exertion ($Q = 82.9$ W m^{-2}) and "moderate" exertion ($Q = 133$ W m^{-2}) under an indoor wind speed ($u = 0.2$ m s^{-1}). These curves are nearly on top of each other: all else equal, a higher metabolic rate will move a person to the right along these curves, but will not substantially alter the curves themselves.

When the apparent temperature T_a is less than 93.3 °C, the time for the core to reach 42 °C is infinite, meaning that the core will equilibrate at a temperature below 42 °C. For T_a above 93.3 °C, the time it takes to reach the fatal core temperature is a function of $\Delta T_a \equiv T_a - 93.3$ °C. Assuming the indoor wind speed, the time it takes to reach a fatal core temperature is nearly independent of the metabolic rate: it takes less than 2 hours if $\Delta T_a \gtrsim 8$ °C and less than 1 hour if $\Delta T_a \gtrsim 20$ °C. The procedure for calculating the time to reach any given core temperature can be found in Lu and Romps (2022).

In the following sections, the apparent temperature will be used to explain the empirical data from Vecellio et al. (2022a), Cottle et al. (2022), and Wolf et al. (2022). It will be shown that a unique apparent temperature of 71.5 °C reliably predicts the varying wet-bulb temperatures at which individuals' core temperatures begin to rise under different levels of exertion. Using an apparent temperature of 93.3 °C, we can predict the temperature and humidity at which the individuals' core temperatures would equilibrate at the fatal value of 42 °C given sustained exposure.

3 Methods

Here, we briefly describe the experiments of Wolf et al. (2022, hereafter, W22) and its companion works (Vecellio et al., 2022a; Cottle et al., 2022). There are two sets of experiments, all conducted indoors. In the first set of experiments, the subjects perform light exertion with an average net metabolic rate of 82.9 W m^{-2}. In the second set, the subjects perform moderate exertion with an average net metabolic rate of 133 W m^{-2}. In each set of experiments, there are six different scenarios. In the first three scenarios, the air temperature T is fixed at about 36°C, 38°C, and 40°C, respectively, while the vapor pressure is gradually increased until the core temperature of the subject starts to rise. In the other three scenarios, the vapor pressure p_v is fixed at around 2.7 kPa, 2.1 kPa and 1.6 kPa, respectively, while the air temperature is gradually increased until the subject's core temperature starts to rise. These 12 empirical combinations of critical (T, p_v) are re-plotted in Figure 3 as black round and triangle symbols. Each symbol represents an average of multiple human subjects and the error bar represents the standard deviation.

To predict these critical (T, p_v) using the heat index model, we plug the actual Q and u into the equation

$$T_a\left(T, p_v, Q, u\right) = 71.5\ ^\circ\mathrm{C}\,, \tag{3}$$

which then defines the critical curve in temperature-humidity space. For any (T, p_v) on this curve, a positive increment of temperature or humidity will force the core temperature to rise above its standard value of 37°. Since there are two different metabolic rates in the experiment – 82.9 W m^{-2} and 133 W m^{-2} – we obtain two curves from equation (3), one for each level of exertion. Regarding the wind speed, although we have written the apparent temperature T_a as a function of u, T_a is really a function of the body's effective heat transfer coefficient (Lu and Romps, 2022). One approach to dealing with this would be to measure the wind speed experimentally and then convert that to a heat transfer coefficient using a theoretical relationship. W22 quotes a wind speed of 0.45 m s^{-1} from previous work (Kenney and Zeman, 2002) that used the same experimental chamber but with different subjects doing more vigorous exercise. Because there is no forced wind in the chamber, the effective wind speed is induced by the movement of the subjects and natural buoyancy-driven convection, and it will depend on body posture (de Dear et al., 1997; Ono et al., 2008; Li and Ito, 2014; Xu et al., 2021). Due to these sources of uncertainty, we take a different approach: we choose the optimal heat transfer coefficient that minimizes the sum of squared differences in vapor pressure between the two curves and the 12 empirical data points. The heat transfer coefficient obtained using this procedure is 3.0 W m^{-2} K^{-1}; a nearly identical value is obtained by minimizing error in temperature instead of vapor pressure. Using the Churchill and Bernstein (1977) relation, this corresponds to a wind speed of 0.2 m s^{-1}, to which we will refer henceforth, with the understanding that it represents a heat transfer coefficient of 3.0 W m^{-2} K^{-1}.

To calculate the survivable limit in the experiments, i.e., the (T, p_v) for which the subjects' core temperatures would have equilibrated at 42 °C, we use the same two metabolic rates (82.9 and 133 W m^{-2}) and the same optimal wind speed (0.2 m s^{-1}). The equation

$$T_a\left(T, p_v, Q, u\right) = 93.3\ ^\circ\mathrm{C} \tag{4}$$

then gives curves in temperature-humidity space that define the survivable limit.

4 Results

The two black curves in Figure 3, labeled by "indoor light" and "indoor moderate," correspond to an apparent temperature of 71.5 °C, with one curve for each exertion level. Despite tuning only a single parameter (the effective wind speed), these curves do a good job of fitting all of the empirical data with two different metabolic rates. The two red curves in Figure 3 correspond to the fatal apparent temperature of 93.3 °C. Comparing curves at the same exertion level, we see that the experiments (black curves) were within 13-16 °C (at constant vapor pressure) or 2.5 kPa (at constant temperature) of the survivable limit (red curves). As discussed in section 2, exposure to conditions beyond the red curves would not immediately bring the core to 42 °C, but would take a length of time that is a function of the exceedance of T_a beyond 93.3 °C.

In addition to the curves of constant apparent temperature, Figure 3 also plots the isopleths of wet-bulb temperature. We see that the indoor light and moderate black curves (apparent temperature = 71.5 °C)

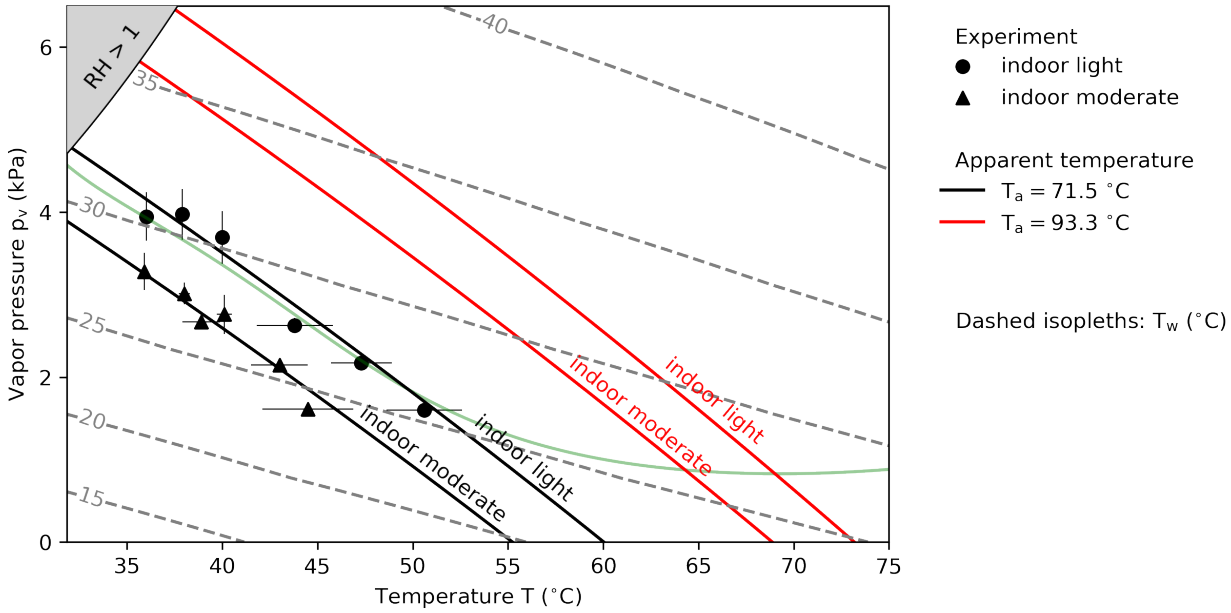

Figure 3: (black symbols) Empirical combinations of temperature and vapor-pressure that cause the core temperature to rise above 37 °C with the indoor wind speed. Light exertion is shown with circles and moderate exertion is shown with triangles. Each symbol represents an average of multiple subjects and the error bar represents the standard deviation. (black curves) Constant apparent temperature of 71.5 °C with the indoor wind speed and light or moderate exertion. (red curves) Same as black curves, but with a constant apparent temperature of 93.3 °C, which leads the core temperature to equilibrate at 42 °C. The indoor wind speed of 0.2 m s^{-1} is chosen using an optimization process as described in section 3. (dashed contours) Isopleths of wet-bulb temperature. (light green curve) The 125 °F isopleth of the NWS polynomial approximation to the heat index, which exhibits unphysical behavior and matches the "indoor light" points only by coincidence as discussed in section 5.

occupy a range of wet-bulb temperature from 20 to 32 °C. This explains the wide spread of critical wet-bulb temperatures recorded by Vecellio et al. (2022a): the core temperature rises at a single apparent temperature of 71.5 °C, but this apparent temperature translates to a range of wet-bulb temperatures. The isopleths of the wet-bulb temperature and the apparent temperature have different slopes in temperature-humidity space, and the apparent-temperature isopleths better explain the empirical data measured by W22. As indicated by the indoor light and moderate red curves (apparent temperature = 93.3°C) in Figure 3, the subjects' core temperatures should equilibrate at 42 °C at wet-bulb temperatures ranging from 24 to 37 °C, compared to the single threshold of 35 °C proposed by Sherwood and Huber (2010).

For a given wind speed, a lower metabolic rate enables a person to endure hotter and more humid conditions. This is consistent with the positions of the "indoor light" and "indoor moderate" curves in temperature-humidity space. As the wind speed is increased, the transfers of sensible and latent heat increasingly dominate the energy balance in equation (1), and we expect the curves of constant core temperature would move upwards and more closely align with curves of constant wet-bulb temperature. Indeed, at the limit of infinite wind speed, the curve corresponding to a constant core temperature of T_c is defined by $T_w = T_c$, as discussed in section 1. Curves obtained in this way would be appropriate for individuals who are outdoors in strong winds.

5 Discussion

We have seen that the apparent temperature is more accurate than the wet-bulb temperature at predicting a human's core temperature. To make this statement quantitative, we can consider the 12 experiments of W22. For each of those experiments, we can use a constant apparent temperature (of 71.5 °C) to predict the wet-bulb temperature at which the core temperature should begin to rise. The errors are then the differences between the predicted and actual wet-bulb temperatures. Likewise, we can use a constant wet-bulb temperature to predict when the core temperature begins to rise. The errors in that method are, again, the differences between the predicted wet-bulb temperature and the actual wet-bulb temperatures.

To ensure a fair comparison, we allow one parameter to be tuned for each prediction method. For the prediction from constant apparent temperature, we tune the wind speed as described in the previous section. Thus, we use 3.0 W m^{-2} K^{-1} (0.2 m s^{-1}). For the prediction from constant wet-bulb temperature, we tune the one free parameter: the constant wet-bulb temperature itself. By minimizing the sum of squared differences between this single wet-bulb temperature and those measured in W22, the optimal value (for predicting a rising core temperature) is found to be 27.6 °C.

Figure 4 plots the observed critical T_w versus the predicted critical T_w using a prediction of single T_w threshold of 27.6 °C (grey symbols) and a single T_a threshold of 71.5 °C (black symbols). The prediction from constant apparent temperature explains 95% of the variance (coefficient of determination $R^2 = 0.95$) while the prediction from constant T_w predicts 0% of the variance. The root-mean-square error of the prediction using a constant apparent temperature is 0.4 °C, compared to 2.0 °C for the prediction using a constant wet-bulb temperature. Thus, we see that the conditions leading to an elevated core temperature are much more accurately predicted using the apparent temperature.

The success of the heat index model in explaining the empirical results of W22 may be compared with previous such efforts. For example, W22 drew two solid curves in their Figure 2 to fit the light-exertion and moderate-exertion data, but those were polynomial fits to the empirical data, and not constructed from a theoretical model (personal communication). In another attempt, Vecellio et al. (2022b) plotted the empirical data alongside the National Weather Service's (NWS) polynomial approximation to the heat index (Rothfusz, 1990). In their Figures 2a and 2d, they plotted isopleths of that polynomial approximation that were intended to correspond to the NWS's definitions of "danger" (an isopleth of 103 °F) and "extreme danger" (an isopleth of 125°F). But there are several problems with that approach. The first problem is that the curves systematically underestimate the danger of moderate exertion (their Figure 2d). The second problem is that a mistake was made in plotting the "danger" curve in their Figures 2a and 2d: if plotted correctly, that "danger" curve would lie far below the empirical data. The third problem is that the "extreme danger" isopleth of that polynomial is outside the region where the polynomial is valid (i.e., outside the region for which the original heat index was defined), and so it is not grounded in any model of physiology and exhibits unrealistic behavior. When we plot that "extreme danger" isopleth of the NWS

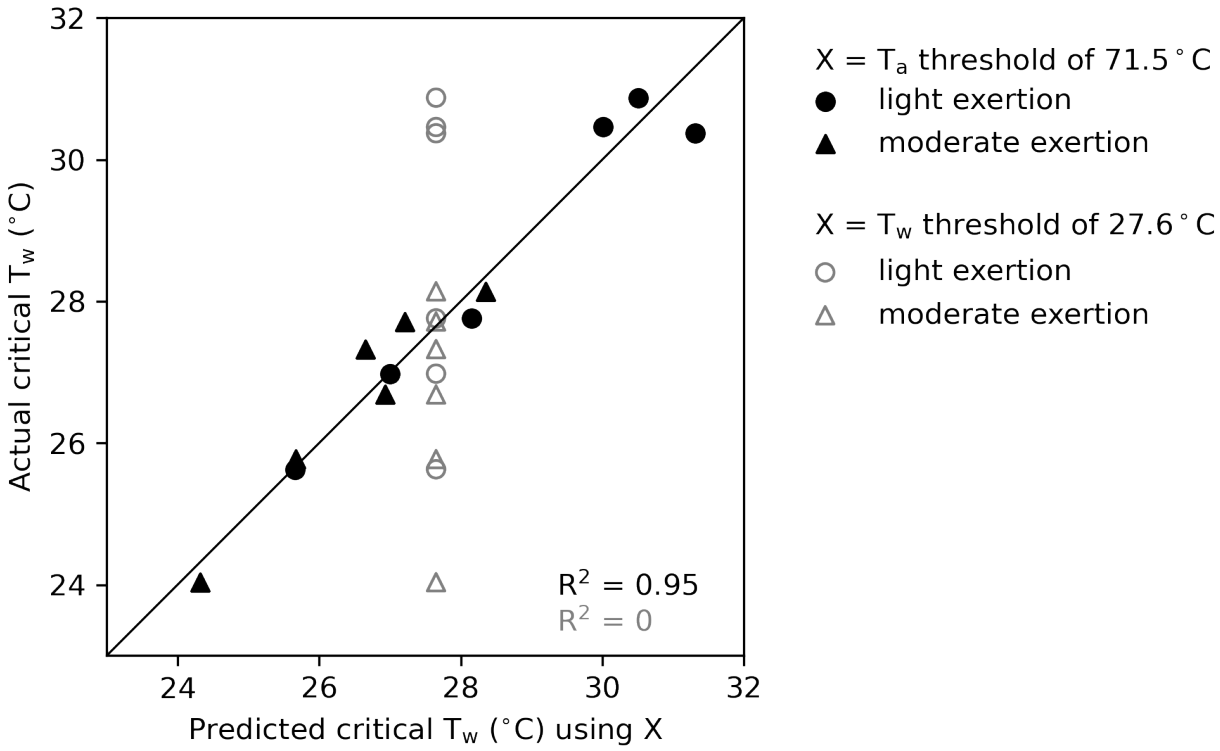

Figure 4: Empirical critical wet-bulb temperatures versus the predicted critical wet-bulb temperature, using (black) apparent temperature of 71.5 °C, and (grey) wet-bulb temperature of 27.6 °C, which is the best-fit value for the present experiment.

approximation in Figure 3 (light green), we see that it happens to coincide with the light-exertion data, but the isopleth bends upward at higher temperatures. In particular, the light green curve is at a minimum vapor pressure at ∼70°C, implying that, at constant vapor pressure, 75 °C is *less* dangerous than 70 °C. In addition, since the NWS's polynomial extrapolation is not based on a physiological model, it is not possible to adapt it to different metabolic rates or wind speeds. In fact, it is just a coincidence that the "extreme danger" curve overlaps the light-exertion data: the physiological model underlying the standard heat index assumes a metabolic rate and wind speed (180 W m^{-2} and 1.5 m s^{-1}) that are far from the conditions in the experiments.

6 Perspective and Significance

The heat index (Steadman, 1979) has been widely used for communicating the danger of high heat and humidity, but little progress has been made in validating its physiological predictions. Quayle and Doehring (1981) divided the heat index into ranges labeled "caution", "extreme caution", "danger", and "extreme danger", and those ranges were adopted by the National Weather Service, but those labels were not based on any peer-reviewed physiological model or laboratory data. In addition, some of the heat index values reported by the National Weather Service have been based on polynomial extrapolation rather than a scientific model, leading those values to be in error by as much as 10 °C (Romps and Lu, 2022). In 2020, a United States administrative judge held that there was no scientific basis to the labels (caution, extreme caution, etc.) applied to the heat index by the National Weather Service (Calhoun, 2020). That decision, which vacated fines imposed against the United States Postal Service (USPS) by the Occupational Safety and Health Administration (OSHA), calls into question OSHA's ability to enforce protections against excessive heat exposure in the workplace in the absence of experimental validation of the heat index (Sapper, 2020). This is the context for the work presented here, which shows that the heat index, appropriately modified to account for the actual wind speed and metabolic rate, can accurately predict the onset of thermoregulatory failure in a laboratory setting.

Acknowledgments

This work was supported by the U.S. Department of Energy's Atmospheric System Research program through the Office of Science's Biological and Environmental Research program under Contract DE-AC02-05CH11231. The authors are grateful to Gregory Barber for a helpful conversation and to three anonymous reviewers for their helpful feedback. Code for calculating the heat index is available in R, Python, and Fortran at `https://romps.berkeley.edu/papers/pubs-2020-heatindex.html`.

Appendix: Sweating rate

The maximum sweating rate for a typical young, healthy, hydrated, and acclimatized adult male is in the range of 1-2 kg hr^{-1} (Adolph and Dill, 1938; Torii, 1995). In Figure 5, we add to Figure 3 the rate of sweat evaporation predicted by the heat-index model at the predicted equilibrium core temperature (which, for light exertion, is 37 °C below and to the left of the "indoor light" black curve, increasing above and to the right of that curve, and hitting 42 °C on the "indoor light" red curve). The sweating rate increases as one moves from the cold and humid region to the hot and dry region. For the experimental data in W22, the predicted sweating rate ranges from 0.2 to 0.6 kg hr^{-1}, which is well below the sweating-rate limit of 1-2 kg hr^{-1}. For all points on the theoretical black curves, the heat-index model predicts a sweating rate at or below 0.8 kg hr^{-1}. For all points on the two red fatal curves, the predicted evaporation rate is equal to about 1 kg hr^{-1} or less. Therefore, the sweating rates predicted by the heat-index model for indoor conditions, even at fatal air temperatures of around 70 °C at zero humidity, are consistent with the maximum sweating rates measured in human subjects.

In this paper, we have referred to the combinations of air temperature, relative humidity, wind speed, and metabolic heat that yield hyperthermia (core temperature starts to rise) and fatality (core equilibrates at 42 °C) by their apparent temperatures of 71.5 and 93.3 °C, respectively. These apparent temperatures

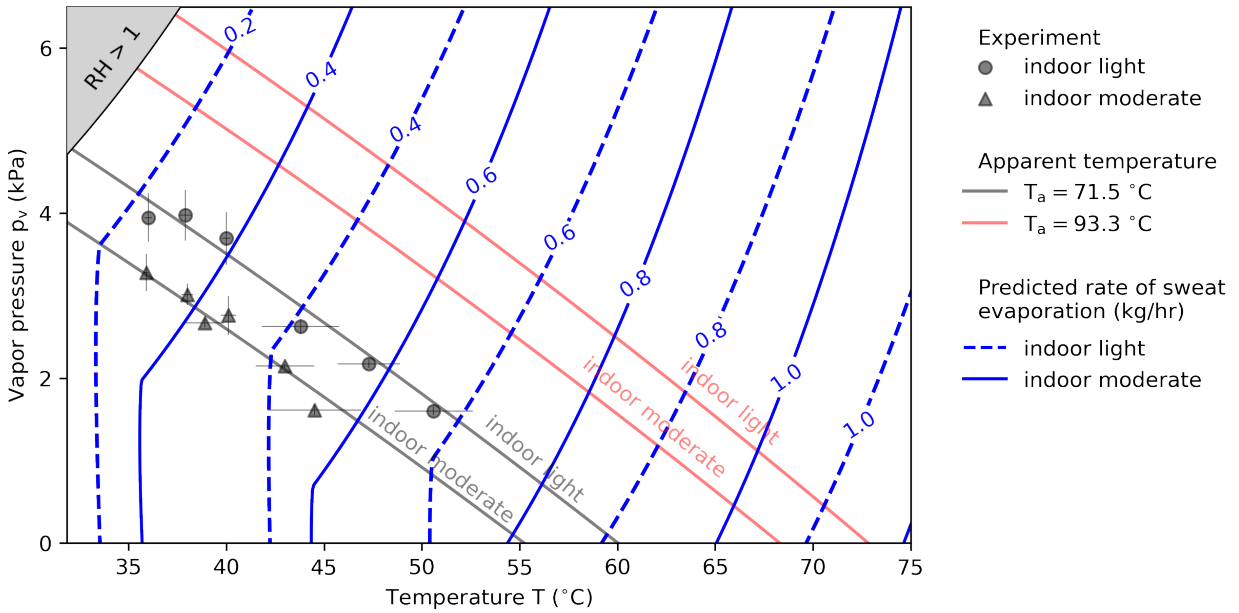

Figure 5: (blue contour) The rate of sweat evaporation predicted by the heat-index model for light (dashed) and moderate (solid) exertions with the indoor wind at the corresponding equilibrium core temperature. The other symbols and curves are explained in the caption of Figure 3.

are the air temperatures in Steadman's reference conditions (water-vapor pressure of 1.6 kPa, an outdoor wind speed of 1.5 m s^{-1}, and metabolic heat of 180 W m^{-2}) that would yield hyperthermia and fatality. At that relatively high reference wind speed of 1.5 m s^{-1}, the predicted rate of sweat evaporation at the equilibrium core temperatures of 37 and 42 °C, respectively, would be 2.4 and 3.4 kg hr^{-1}, respectively. These sweating rates exceed the typical maximum rate reported in the literature of 1-2 kg hr^{-1}. For a real human to perform the same as in the idealized heat-index model in those extreme outdoor conditions, a misting fan would likely be needed to keep the skin surface wet. Without a misting fan, a person under Steadman's reference (outdoor) conditions would suffer from hyperthermia and fatality at air temperatures lower than 71.5 and 93.3 °C, respectively. Since, for an indoor wind speed, the sweating rate predicted by the heat-index model is below the empirical maximum, the heat-index model is accurate for indoor conditions without a misting fan.

References

Adolph, E. F. and D. B. Dill, 1938: Observations on water metabolism in the desert. *American Journal of Physiology-Legacy Content*, **123 (2)**, 369–378.

Bouchama, A. and J. P. Knochel, 2002: Heat stroke. *New England Journal of Medicine*, **346 (25)**, 1978–1988.

Calhoun, S. D., 2020: Secretary of Labor v. United States Postal Service, National Association of Letter Carriers (NALC) and National Rural Letter Carriers' Association (NRLCA). Tech. Rep. OSHRC Docket No. 16-1713, Occupational Safety and Health Review Commission. URL `https://www.oshrc.gov/assets/1/6/16-1713_Decision_and_Order_-_dated.html`.

Churchill, S. W. and M. Bernstein, 1977: A Correlating Equation for Forced Convection From Gases and Liquids to a Circular Cylinder in Crossflow. *Journal of Heat Transfer*, **99 (2)**, 300–306, doi:10.1115/1.3450685, URL `https://doi.org/10.1115/1.3450685`.

Coffel, E. D., R. M. Horton, and A. D. Sherbinin, 2018: Temperature and humidity based projections of

a rapid rise in global heat stress exposure during the 21st century. *Environmental Research Letters*, **13**, doi:10.1088/1748-9326/aaa00e.

Cottle, R. M., S. T. Wolf, Z. S. Lichter, and W. L. Kenney, 2022: Validity and reliability of a protocol to establish human critical environmental limits (psu heat project). *Journal of Applied Physiology*, **132**, 334–339, doi:10.1152/japplphysiol.00736.2021.

de Dear, R. J., E. Arens, Z. Hui, and M. Oguro, 1997: Convective and radiative heat transfer coefficients for individual human body segments. *International Journal of Biometeorology*, **40 (3)**, 141–156, doi:10.1007/s004840050035, URL `https://doi.org/10.1007/s004840050035`.

Gostimirovic, M., R. Novakovic, J. Rajkovic, V. Djokic, D. Terzic, S. Putnik, and L. Gojkovic-Bukarica, 2020: The influence of climate change on human cardiovascular function. *Archives of Environmental & Occupational Health*, **75 (7)**, 406–414.

Im, E. S., S. Kang, and E. A. Eltahir, 2018: Projections of rising heat stress over the western maritime continent from dynamically downscaled climate simulations. *Global and Planetary Change*, **165**, 160–172, doi:10.1016/j.gloplacha.2018.02.014.

Im, E.-S., J. S. Pal, and E. A. B. Eltahir, 2017: Deadly heat waves projected in the densely populated agricultural regions of south asia. *Science Advances*, **3 (8)**, e1603 322, doi:10.1126/sciadv.1603322, URL `https://www.science.org/doi/abs/10.1126/sciadv.1603322`, `https://www.science.org/doi/pdf/10.1126/sciadv.1603322`.

Kenney, W. L. and M. J. Zeman, 2002: Psychrometric limits and critical evaporative coefficients for unacclimated men and women. *Journal of Applied Physiology*, **92 (6)**, 2256–2263.

Li, C. and K. Ito, 2014: Numerical and experimental estimation of convective heat transfer coefficient of human body under strong forced convective flow. *Journal of Wind Engineering and Industrial Aerodynamics*, **126**, 107–117, doi:10.1016/j.jweia.2014.01.003.

Lu, Y.-C. and D. M. Romps, 2022: Extending the heat index. *Journal of Applied Meteorology and Climatology*, **61 (10)**, 1367–1383.

Monteiro, J. M. and R. Caballero, 2019: Characterization of extreme wet-bulb temperature events in southern pakistan. *Geophysical Research Letters*, **46**, 10 659–10 668, doi:10.1029/2019GL084711.

Nybo, L. and J. González-Alonso, 2015: Critical core temperature: a hypothesis too simplistic to explain hyperthermia-induced fatigue. *Scandinavian Journal of Medicine & Science in Sports*, **25 (S1)**, 4–5, doi:https://doi.org/10.1111/sms.12444, URL `https://onlinelibrary.wiley.com/doi/abs/10.1111/sms.12444`, `https://onlinelibrary.wiley.com/doi/pdf/10.1111/sms.12444`.

Ono, T., S. Murakami, R. Ooka, and T. Omori, 2008: Numerical and experimental study on convective heat transfer of the human body in the outdoor environment. *Journal of Wind Engineering and Industrial Aerodynamics*, **96**, 1719–1732, doi:10.1016/j.jweia.2008.02.007.

Pal, J. S. and E. A. Eltahir, 2016: Future temperature in southwest asia projected to exceed a threshold for human adaptability. *Nature Climate Change*, **6**, 197–200, doi:10.1038/nclimate2833.

Quayle, R. and F. Doehring, 1981: Heat stress: A comparison of indices. *Weatherwise*, **34 (3)**, 120–124.

Ramsay, E. E., G. M. Fleming, P. A. Faber, S. F. Barker, R. Sweeney, R. R. Taruc, S. L. Chown, and G. A. Duffy, 2021: Chronic heat stress in tropical urban informal settlements. *iScience*, **24**, doi:10.1016/j.isci.2021.103248.

Raymond, C., T. Matthews, and R. M. Horton, 2020: The emergence of heat and humidity too severe for human tolerance. *Science Advances*, **6 (19)**, eaaw1838.

Rogers, C. D., M. Ting, C. Li, K. Kornhuber, E. D. Coffel, R. M. Horton, C. Raymond, and D. Singh, 2021: Recent increases in exposure to extreme humid-heat events disproportionately affect populated regions. *Geophysical Research Letters*, **48**, doi:10.1029/2021GL094183.

Romps, D. M. and Y.-C. Lu, 2022: Chronically underestimated: a reassessment of US heat waves using the extended heat index. *Environmental Research Letters*, **17 (9)**, 094 017.

Rothfusz, L. P., 1990: The Heat Index "equation" (or, more than you ever wanted to know about Heat Index). Technical Attachment SR 90-23, NWS Southern Region Headquarters, Forth Worth, TX.

Saeed, F., C. F. Schleussner, and M. Ashfaq, 2021: Deadly heat stress to become commonplace across south asia already at 1.5°c of global warming. *Geophysical Research Letters*, **48**, doi:10.1029/2020GL091191.

Sapper, A. G., 2020: An emperor without clothes: No scientific basis to rely on NWS heat index chart. *Professional Safety*, **65 (9)**, 22–23.

Schär, C., 2016: Climate extremes: The worst heat waves to come. *Nature Climate Change*, **6**, 128–129, doi:10.1038/nclimate2864.

Sherwood, S. C., 2018: How important is humidity in heat stress? *Journal of Geophysical Research: Atmospheres*, **123 (21)**, 11,808–11,810, doi:https://doi.org/10.1029/2018JD028969, URL `https://agupubs.onlinelibrary.wiley.com/doi/abs/10.1029/2018JD028969`, `https://agupubs.onlinelibrary.wiley.com/doi/pdf/10.1029/2018JD028969`.

Sherwood, S. C. and M. Huber, 2010: An adaptability limit to climate change due to heat stress. *Proceedings of the National Academy of Sciences*, **107 (21)**, 9552–9555.

Steadman, R. G., 1979: The assessment of sultriness. Part I: A temperature-humidity index based on human physiology and clothing science. *Journal of Applied Meteorology*, **18 (7)**, 861–873, doi:10.1175/1520-0450(1979)018⟨0861:TAOSPI⟩2.0.CO;2.

Stolwijk, J. A. J. and J. D. Hardy, 1966: Temperature regulation in man —a theoretical study. *Pflüger's Archiv für die gesamte Physiologie des Menschen und der Tiere*, **291 (2)**, 129–162, doi:10.1007/BF00412787, URL `https://doi.org/10.1007/BF00412787`.

Torii, M., 1995: Maximal sweating rate in humans. *Journal of Human Ergology*, **24 (2)**, 137–152.

Vecellio, D. J., S. T. Wolf, R. M. Cottle, and W. L. Kenney, 2022a: Evaluating the 35c wet-bulb temperature adaptability threshold for young, healthy subjects (psu heat project). *Journal of Applied Physiology*, **132**, 340–345, doi:10.1152/japplphysiol.00738.2021.

Vecellio, D. J., S. T. Wolf, R. M. Cottle, and W. L. Kenney, 2022b: Utility of the heat index in defining the upper limits of thermal balance during light physical activity (PSU HEAT project). *International Journal of Biometeorology*, doi:10.1007/s00484-022-02316-z, URL `https://doi.org/10.1007%2Fs00484-022-02316-z`.

Wolf, S. T., R. M. Cottle, D. J. Vecellio, and W. L. Kenney, 2022: Critical environmental limits for young, healthy adults (psu heat project). *Journal of Applied Physiology*, **132**, 327–333, doi:10.1152/japplphysiol.00737.2021.

Xu, J., A. Psikuta, J. Li, S. Annaheim, and R. M. Rossi, 2021: Evaluation of the convective heat transfer coefficient of human body and its effect on the human thermoregulation predictions. *Building and Environment*, **196**, doi:10.1016/j.buildenv.2021.107778.